

Parametric co-linear axion photon instability

K. A. Beyer,^{1,*} G. Marocco,^{1,†} C. Danson,^{2,3} R. Bingham,^{4,5} and G. Gregori¹

¹*Department of Physics, University of Oxford, Parks Road, Oxford OX1 3PU, UK*

²*AWE, Aldermaston, Reading RG7 4PR, UK*

³*OxCHEDS, Clarendon Laboratory, Department of Physics, University of Oxford, UK*

⁴*Rutherford Appleton Laboratory, Chilton, Didcot OX11 0QX, UK*

⁵*Department of Physics, University of Strathclyde, Glasgow G4 0NG, UK*

Axions and axion-like particles generically couple to QED via the axion-photon-photon interaction. This leads to a modification of Maxwell's equations known in the literature as axion-electrodynamics. The new form of Maxwell's equations gives rise to a new parametric instability in which a strong pump decays into a scattered light wave and an axion. This axion mode grows exponentially in time and leads to a change in the polarisation of the initial laser beam, therefore providing a signal for detection. Currently operating laser systems can put bounds on the axion parameter space, however longer pulselengths are necessary to reach the current best laboratory bounds of light-shining through wall experiments.

I. INTRODUCTION

Despite the many successes of the Standard Model, it is thought to be incomplete. The strong sector of the Standard Model allows CP violation, which is constrained to cancel the electroweak contribution by measurements of the electromagnetic dipole moment of the neutron [1, 2]. This is known as the strong CP problem, which can be solved in an elegant fashion by introducing a new chiral, anomalous $U(1)_{\text{PQ}}$ symmetry, as pointed out by Peccei and Quinn [3, 4]. Such global symmetry, after spontaneously breaking at a high scale, dynamically drives the CP violating parameter $\bar{\theta}$ to 0. The pseudo Nambu-Goldstone boson originating from the symmetry breaking process is called the axion [5, 6]. It was pointed out that axion models can account for the dark matter content of the universe [7–9]. Axion-like particles (ALPs) may abundantly arise in extensions of the Standard Model, such as the low energy spectrum of String Theory [10, 11]. In the following we will use the term axion to refer to both, the CP restoring QCD axion and ALPs.

Axions generically couple to Standard Model photons via a dimension 5 operator

$$\mathcal{L}_{a\gamma\gamma} = g_{a\gamma\gamma} a \mathbf{E} \cdot \mathbf{B}. \quad (1)$$

with a coupling strength parametrized by $g_{a\gamma\gamma}$. The inclusion of equation 1 modifies Maxwell's equations [12]. Axion electrodynamics in vacuum has been widely applied to axion detection experiments (for a review see, e.g., [13]). A range of phenomena like the axion-photon mass mixing in magnetic field backgrounds [14, 15] or axion sourced birefringence [16] are extensively studied in the literature.

The propagation of an intense laser beam receives corrections due to the presence of axions. As was investi-

gated by the PVLAS collaboration, axions source birefringence [17] of light propagating through a strong constant magnetic field. This is a consequence of the altered dispersion relation [15]. In this work we extend previous analyses to look at systems in plane-wave backgrounds. We will demonstrate the existence of a new parametric decay instability of one photon in the seed pulse into an axion and a secondary photon, satisfying

$$\omega_0 = \omega_\gamma + \omega_a \quad \text{and} \quad \mathbf{k}_0 = \mathbf{k}_\gamma + \mathbf{k}_a. \quad (2)$$

Here, subscript γ denotes the scattered photon and a the axion. Physically, small fluctuations in the axion field source electromagnetic fields. Such fields then interact with the pump pulse and source the axion field. Hence, a positive feedback is generated which leads to the growth of the axion fluctuations. A similar idea was investigated in [18] for the case of parametric excitation of axions, where a different ansatz is used for the time-dependence of the fields. Additionally, the stimulated decay of photons (or more specifically, plasmons) into axions have been considered in [19].

The polarisation-dependent coupling (1) forces the scattered mode to have a polarisation orthogonal to the seed pulse. Hence, the laser polarisation depletes. This rate of polarisation change scales as $g_{a\gamma\gamma}$, as opposed to the $g_{a\gamma\gamma}^2$ scaling of conventional birefringence or dichroism experiments [16].

This paper is organised as follows: In section II we derive the set of equations coupling the axion to electrodynamics in a strong pump background and combine them to find the dispersion relation of the system. In section III we solve the dispersion relation. For simplicity we limit our analysis to the co-linear limit and leave the general treatment for a later paper. In section IV we comment on the significance of this axion-photon instability. Within the paper we employ natural units with $\hbar = c = k_B = 4\pi\epsilon_0 = 1$.

* Authors to whom correspondence should be addressed: konstantin.beyer@physics.ox.ac.uk

† giacomo.marocco@physics.ox.ac.uk

II. AXION-PHOTON DISPERSION RELATION

The axion-photon vertex (1) introduces a source and current to the vacuum Maxwell's equations [12, 14]

$$\begin{aligned}\nabla \cdot \mathbf{E} &= g_{a\gamma\gamma} (\nabla a) \cdot \mathbf{B}, \\ \nabla \cdot \mathbf{B} &= 0, \\ \nabla \times \mathbf{E} &= -\partial_t \mathbf{B}, \\ \nabla \times \mathbf{B} &= \partial_t \mathbf{E} + g_{a\gamma\gamma} (\mathbf{E} \times \nabla a - \mathbf{B} \partial_t a).\end{aligned}\quad (3)$$

The electric and magnetic fields in the axion photon coupling term (1) are defined as

$$\begin{aligned}\mathbf{E} &= -\partial_t \mathbf{A} - \nabla \phi, \\ \mathbf{B} &= \nabla \times \mathbf{A}.\end{aligned}\quad (4)$$

We employ Coulomb gauge $\nabla \cdot \mathbf{A} = 0$, and work in the *colinear* limit where all momenta, are parallel to find the wave equations for the gauge potentials

$$(\partial_t^2 - \nabla^2) \mathbf{A} = g_{a\gamma\gamma} \nabla \times (a \partial_t \mathbf{A}) \quad (5)$$

and

$$\nabla^2 \phi = 0. \quad (6)$$

In this colinear limit, we may use the residual gauge freedom to set $\phi = 0$. The remaining equation of motion for the axion is then

$$(\partial_t^2 - \nabla^2 + m_a^2) a = g_{a\gamma\gamma} (\partial_t \mathbf{A}) \cdot (\nabla \times \mathbf{A}). \quad (7)$$

We perform a linear stability analysis by setting

$$\mathbf{A} = \mathbf{A}_0 \cos(\omega_0 t - \mathbf{k}_0 \cdot \mathbf{x}) + \tilde{\mathbf{A}}, \quad a = \tilde{a}, \quad (8)$$

where $\tilde{\mathbf{A}}, \tilde{a} \ll \mathbf{A}_0$. Note that this assumption is only valid for early times before the instability turns strongly non-linear. To solve this system of coupled partial differential equations, we first perform a spatial Fourier transform of all fields

$$f(\mathbf{k}, t) \equiv \int f(\mathbf{x}, t) e^{-i\mathbf{k} \cdot \mathbf{x}} \frac{d^3 \mathbf{x}}{(2\pi)^{3/2}} \quad (9)$$

to find a coupled set of linearised ordinary differential equations

$$(-\partial_t^2 - \mathbf{k}^2) \tilde{\mathbf{A}}(\mathbf{k}, t) = -g_{a\gamma\gamma} \frac{\omega_0}{2} (\mathbf{k} \times \mathbf{A}_0) (\tilde{a}_- e^{-i\omega_0 t} - \tilde{a}_+ e^{i\omega_0 t}), \quad (10)$$

$$(-\partial_t^2 - \mathbf{k}^2 - m_a^2) \tilde{a}(\mathbf{k}, t) = \frac{g_{a\gamma\gamma}}{2} \mathbf{A}_0 \cdot \left[e^{i\omega_0 t} (\omega_0 \mathbf{k}_+ - i\mathbf{k}_0 \partial_t) \times \tilde{\mathbf{A}}_+ - e^{-i\omega_0 t} (\omega_0 \mathbf{k}_- - i\mathbf{k}_0 \partial_t) \times \tilde{\mathbf{A}}_- \right]. \quad (11)$$

with subscript \pm denoting the dependency on $\mathbf{k} \pm \mathbf{k}_0$.

To analyse the coupled system's behaviour we make an Ansatz for the temporal dependency of the fields

$$f(\mathbf{k}, t) = f(\mathbf{k}) e^{-i\omega(\mathbf{k})t} \quad (12)$$

which reduces the differential equations (10) and (11) to algebraic equations in the fields. They are solved for frequencies satisfying the dispersion relation

$$D^a(\omega, k) = \frac{g_{a\gamma\gamma}^2 A_0^2}{4} \omega_0 (\omega_0 k - \omega(k) k_0) \left(\frac{k_-}{D_-^\gamma} + \frac{k_+}{D_+^\gamma} \right), \quad (13)$$

where $k = |\mathbf{k}|$, $D^a(\omega, k) \equiv \omega^2 - k^2 - m_a^2$, $D_\pm^\gamma \equiv (\omega \pm \omega_0)^2 - (k \pm k_0)^2$, and functions of $(\omega \pm 2\omega_0, \mathbf{k} \pm 2\mathbf{k}_0)$ are neglected as off-resonant and hence sub-dominant.

The rest of the paper is concerned with an investigation of this dispersion relation.

III. GROWTH RATE

We would now like to solve equation (13) for real k , while allowing complex ω . The dispersion relation is a 6th-order polynomial in ω . Immediately the two real roots $\omega(k) = k$ can be discarded in the following as we are interested in unstable modes. Such unstable modes are characterised by a complex frequency with non-vanishing imaginary part $\Gamma \equiv \Im(\omega)$ which defines the growth rate. We proceed by working with the remaining 4th-order polynomial and splitting ω into its real and imaginary parts $\omega(k) = \omega_a(k) + i\Gamma(k)$ for $\omega_a(k), \Gamma \in \mathcal{R}$. The resulting real and imaginary equations are linearly independent and must be satisfied individually.

The imaginary equation is a cubic polynomial in the growth rate Γ with one trivial solution $\Gamma = 0$ and two non-trivial ones

$$\Gamma = \pm \sqrt{\frac{3k\omega_a^2 + 2\omega_a^3 - 4\omega_a\omega_0^2 - k^3 - m_a^2(\omega_a + k) + g_{a\gamma\gamma}^2 A_0^2 k \omega_0^2}{k - 2\omega_a}}. \quad (14)$$

From our ansatz (12) we know that a positive Γ corresponds to growth, hence we focus only on the positive root. After substitution of Γ into the real part of the equation we are then left with a single algebraic equation for $\omega_a(k)$. Figure 1 shows that in our case, the frequency $\omega_a(k)$ is very small and thus motivating an expansion in ω_a , which we find to be

$$\omega_a(k) = k \frac{(g_{a\gamma\gamma} A_0)^2}{16} \left((g_{a\gamma\gamma} A_0)^2 - \left(\frac{m_a}{\omega_0} \right)^2 \right). \quad (15)$$

Here we dropped terms of order 6 in $(g_{a\gamma\gamma} A_0)$, (m_a/ω_0) and k as being small. We may then express the growth rate as

$$\Gamma(k) = \omega_0 \sqrt{(g_{a\gamma\gamma} A_0)^2 - \left(\frac{m_a}{\omega_0} \right)^2 - \left(\frac{k}{k_0} \right)^2}, \quad (16)$$

where we have again dropped higher order terms in $(g_{a\gamma\gamma} A_0)$, (m_a/ω_0) and (k/k_0) .

Upon a closer look at (16) the qualitative behaviour of the numerical solution depicted in fig 1 is recovered. We find growth below a cutoff in k which is defined by

$$k_{\text{cutoff}} = k_0 \sqrt{(g_{a\gamma\gamma} A_0)^2 - \left(\frac{m_a}{\omega_0} \right)^2} \quad (17)$$

at which point Γ becomes imaginary and our solution breaks down. The growth rate is essentially constant in $k < k_{\text{cutoff}}$ and in the following we will suppress the dependence of Γ . (16) also reveals a second cutoff for $m_a/\omega_0 > g_{a\gamma\gamma} A_0$ above which no instability is found.

From (15) we know the phase velocity of the unstable modes

$$v_a = \frac{\partial \omega_a(k)}{\partial k} = \frac{(g_{a\gamma\gamma} A_0)^2}{16} \left((g_{a\gamma\gamma} A_0)^2 - \left(\frac{m_a}{\omega_0} \right)^2 \right), \quad (18)$$

which can be much less than the speed of light even for massless $m_a = 0$ axions.

IV. DISCUSSION AND APPLICATION

A possible search experiment based on the above discussion utilises lasers to drive the instability. The frequency of any growing axion mode is very small and thus does not greatly affect the frequency or total energy of the pump beam. The most suitable observable is instead the polarisation of the pump beam. By the nature of the $\mathbf{E} \cdot \mathbf{B}$ coupling, any seed-photon which decays into an axion, will also produce a photon of opposite polarisation.

The set-up in mind consists of a pump pulse polarised in \hat{x} and a weaker probe with polarisation in \hat{y} . We define the initial polarisation of the combined wave as

$$\mathcal{P}(0) = \frac{\mathbf{A} \cdot \hat{x} - \mathbf{A} \cdot \hat{y}}{A_0} \equiv 1 - \varepsilon. \quad (19)$$

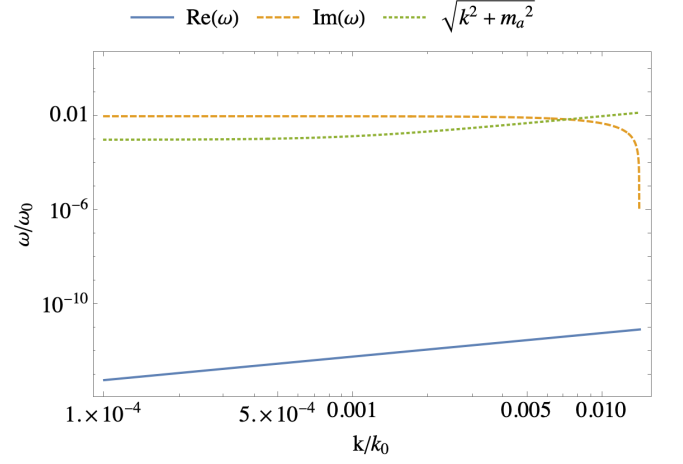


FIG. 1. The plot shows the growing solution to the dispersion relation (13). The blue solid curve shows the real part $\omega_a(k)$ corresponding to the modes frequency while the dashed yellow curve depicts the growth rate Γ . Note that here we included the $\mathcal{O}(k^2)$ contributions to show the cutoff. As a reference we include the vacuum dispersion relation for an axion with the same mass in dotted green. For illustration purposes we have chosen $m_a/\omega_0 = 10^{-2}$ and $g_{a\gamma\gamma} A_0 = 10^{-3}$. We see that even for such large values, the axion frequency is negligibly small.

Here, $\varepsilon = A_0/\tilde{A}$. For early times, the pump pulse is unaffected and only the probe grows together with the axion mode

$$\tilde{A}(\mathbf{k}, t) = \tilde{A}(\mathbf{k}, 0) e^{-i\omega_0 t + \Gamma t} \quad (20)$$

where we ignore the small shift in frequency as $\omega_a(k) \ll \omega_0$. Since the growth rate does not depend on k , the Fourier transform is trivial. Thus, the polarisation has a time dependence given by

$$\mathcal{P}(t) = 1 - \varepsilon e^{\Gamma t}. \quad (21)$$

We immediately see that the most important part is the exponential. The timescale of growth t will be set by the laser pulse length τ . The growth rate (16) depends on the laser parameters

$$\Gamma = 3 \times 10^7 \text{ s}^{-1} \left(\frac{g_{a\gamma\gamma}}{10^{-8} \text{ GeV}^{-1}} \right) \left(\frac{\mathcal{I}}{10^{23} \text{ W/cm}^2} \right)^{\frac{1}{2}}. \quad (22)$$

The intensity achievable depends on the focal spot size and must be maintained for long enough distances to encompass the wavelength of the unstable axion mode $\lambda_a \geq k_{\text{cutoff}}^{-1}$. We can estimate that distance by

$$\lambda_a \geq 10 \text{ m} \left(\frac{g_{a\gamma\gamma}}{10^{-8} \text{ GeV}^{-1}} \right)^{-1} \left(\frac{\mathcal{I}}{10^{23} \text{ W/cm}^2} \right)^{-\frac{1}{2}} \quad (23)$$

The highest laser intensity currently running systems can generate is around $\mathcal{I} = 10^{23} \text{ W/cm}^2$ and lasts for $\tau = 10 \text{ fs}$ [20]; for a review of current laser technology see [21]. Such intensities would correspond to a wavelength

of $\lambda_a = 9$ m. Generating and maintaining long laser focuses might be possible with a variety of approaches in the future. For example, recent plasma-waveguides are capable of maintaining a laser focus over 10 m scales [22, 23]. It is also worth pointing out that the focus length decreases mildly with laser power, hence the problem will become marginally simpler in the future. We will for now

assume that a sufficiently long focus can be generated to proceed.

The e-folding time is readily found from (22) and must be compared to the pulselength of a $\mathcal{I} = 10^{23}$ W/cm² pulse which lasts for $\tau \sim 10$ fs. This restricts the couplings we can probe, assuming we are capable of measuring a polarisation change $\Delta\mathcal{P}$, by inverting (21) we find

$$g_{a\gamma\gamma} \geq 3.4 \times 10^{-2} \text{ GeV}^{-1} \left(\frac{\mathcal{I}}{10^{23} \text{ W/cm}^2} \right)^{-\frac{1}{2}} \left(\frac{\tau}{10 \text{ fs}} \right)^{-1} \ln \left[\frac{\Delta\mathcal{P}}{\varepsilon} + 1 \right]. \quad (24)$$

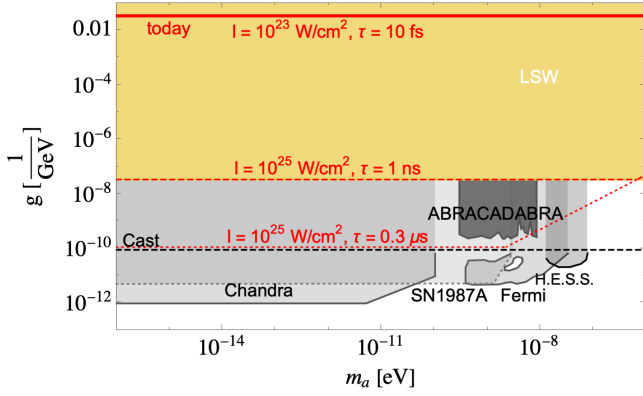


FIG. 2. Axion exclusion plot indicating past experiments and the current work. The coloured regions correspond to purely laboratory based experiments while in grey-scale we indicate astrophysical and dark matter bounds. In yellow results from light-shining through wall experiments are shown [24, 25]. The dark grey region is excluded by the ABRACADABRA collaboration [26] looking for dark matter axions. The dashed black line indicates CAST constraints [27]. The lighter grey regions are excluded by the Chandra telescope [28], observations made on the SN1987A supernova [29], the Fermi LAT collaboration [30] and considerations of a Hot Neutron Star in HESS J1731-347 [31]. The solid red line indicates the reach of an experiment as described in the main text with laser intensities of $\mathcal{I} = 10^{23}$ W/cm² with pulselength $\tau = 10$ fs. The dashed and dotted red lines indicate the laser requirements to reach bounds similar to LSW and CAST respectively.

The log gives an $\mathcal{O}(1)$ contribution, it is not inconceivable to measure $\Delta\mathcal{P} \sim 0.01$. We also note that the axion wavelength for such couplings decreases to $3 \mu\text{m}$, a length scale which is very close to the $1.1 \mu\text{m}$ spot-size of [20]. We therefore conclude that such couplings could be measured today.

The instability cuts off at large masses, hence we are only sensitive to masses satisfying

$$m_a \leq 2 \times 10^{-8} \text{ eV} \left(\frac{g_{a\gamma\gamma}}{10^{-8} \text{ GeV}^{-1}} \right) \left(\frac{\mathcal{I}}{10^{23} \text{ W/cm}^2} \right)^{\frac{1}{2}}. \quad (25)$$

We find that such an approach would reach bounds as indicated by the red line in fig. 2. While the bounds are within the exclusion region of LSW experiments it is worth stressing that our bounds on $g_{a\gamma\gamma}$ grow with laser energy and pulse length. To reach current LSW bounds, we would need to extend the duration of the high intensity pulse to 10 ns (without increasing the intensity). Such long pulses are possible, however not currently in combination with high intensities.

It is worth mentioning that this approach can, unfortunately, not be used to probe the QCD axion. Here the coupling and mass are no longer independent but rather $g_{a\gamma\gamma} \propto m_a$. To reach this we would need laser fields above the Schwinger critical field limit.

Another possible application of the axion-photon instability described in this paper is within astrophysics. The very long wavelength of the unstable mode naturally lends itself to macroscopic distances as are usually encountered in astrophysics. Possible applications remain to be investigated.

We would also like to point out that working beyond the perfect phase-matching condition (2) may lead to an enhanced signal. A phase mismatch may allow shorter wavelengths to become unstable, thus providing a measurable signal in laboratory experiments, at the expense of a lower growth rate. This possibility is left for future work.

ACKNOWLEDGMENTS

The research leading to these results has received funding from AWE plc. British Crown Copyright 2021/AWE.

-
- [1] C. A. Baker et al. An Improved experimental limit on the electric dipole moment of the neutron. *Phys. Rev. Lett.*, 97:131801, 2006.
- [2] J. M. Pendlebury et al. Revised experimental upper limit on the electric dipole moment of the neutron. *Phys. Rev.*, D92(9):092003, 2015.
- [3] R. D. Peccei and Helen R. Quinn. CP conservation in the presence of pseudoparticles. *Phys. Rev. Lett.*, 38:1440–1443, Jun 1977.
- [4] R. D. Peccei and Helen R. Quinn. Constraints imposed by CP conservation in the presence of pseudoparticles. *Phys. Rev. D*, 16:1791–1797, Sep 1977.
- [5] Steven Weinberg. A New Light Boson? *Phys. Rev. Lett.*, 40:223–226, 1978.
- [6] Frank Wilczek. Problem of Strong P and T Invariance in the Presence of Instantons. *Phys. Rev. Lett.*, 40:279–282, 1978.
- [7] John Preskill, Mark B. Wise, and Frank Wilczek. Cosmology of the Invisible Axion. *Phys. Lett.*, 120B:127–132, 1983.
- [8] L. F. Abbott and P. Sikivie. A Cosmological Bound on the Invisible Axion. *Phys. Lett.*, 120B:133–136, 1983.
- [9] Michael Dine and Willy Fischler. The Not So Harmless Axion. *Phys. Lett.*, 120B:137–141, 1983.
- [10] Edward Witten. Some Properties of $O(32)$ Superstrings. *Phys. Lett.*, 149B:351–356, 1984.
- [11] Asimina Arvanitaki, Savas Dimopoulos, Sergei Dubovsky, Nemanja Kaloper, and John March-Russell. String Axiverse. *Phys. Rev.*, D81:123530, 2010.
- [12] Frank Wilczek. Two Applications of Axion Electrodynamics. *Phys. Rev. Lett.*, 58:1799, 1987.
- [13] Pierre Sikivie. Invisible Axion Search Methods. 3 2020.
- [14] P. Sikivie. Experimental Tests of the Invisible Axion. *Phys. Rev. Lett.*, 51:1415–1417, 1983. [Erratum: *Phys.Rev.Lett.* 52, 695 (1984)].
- [15] Georg Raffelt and Leo Stodolsky. Mixing of the Photon with Low Mass Particles. *Phys. Rev.*, D37:1237, 1988.
- [16] L. Maiani, R. Petronzio, and E. Zavattini. Effects of nearly massless, spin-zero particles on light propagation in a magnetic field. *Physics Letters B*, 175(3):359–363, August 1986.
- [17] Federico Della Valle, Aldo Ejlli, Ugo Gastaldi, Giuseppe Messineo, Edoardo Milotti, Ruggero Pengo, Giuseppe Ruoso, and Guido Zavattini. The PVLAS experiment: measuring vacuum magnetic birefringence and dichroism with a birefringent Fabry-Perot cavity. *Eur. Phys. J.*, C76(1):24, 2016.
- [18] J. T. Mendonca. Axion excitation by intense laser fields. *EPL*, 79(2):21001, 2007.
- [19] Georg G. Raffelt. Plasmon decay into low-mass bosons in stars. *Phys. Rev. D*, 37(6):1356–1359, March 1988.
- [20] Jin Woo Yoon, Yeong Gyu Kim, Il Woo Choi, Jae Hee Sung, Hwang Woon Lee, Seong Ku Lee, and Chang Hee Nam. Realization of laser intensity over 10^{23} W/cm^2 . *Optica*, 8(5):630–635, May 2021.
- [21] Colin N. Danson, Constantin Haefner, Jake Bromage, Thomas Butcher, Jean-Christophe F. Chanteloup, Enam A. Chowdhury, Almantas Galvanauskas, Leonida A. Gizzi, Joachim Hein, David I. Hillier, and et al. Petawatt and exawatt class lasers worldwide. *High Power Laser Science and Engineering*, 7:54, 2019.
- [22] R. J. Shalloo, C. Arran, A. Picksley, A. von Boetticher, L. Corner, J. Holloway, G. Hine, J. Jonnerby, H. M. Milchberg, C. Thornton, R. Walczak, and S. M. Hooker. Low-density hydrodynamic optical-field-ionized plasma channels generated with an axicon lens. *Physical Review Accelerators and Beams*, 22(4):041302, April 2019.
- [23] A. Picksley et al. Meter-Scale, Conditioned Hydrodynamic Optical-Field-Ionized Plasma Channels. *Phys. Rev. E*, 102(5):053201, 2020.
- [24] Klaus Ehret et al. New ALPS Results on Hidden-Sector Lightweights. *Phys. Lett. B*, 689:149–155, 2010.
- [25] R. Ballou et al. New exclusion limits on scalar and pseudoscalar axionlike particles from light shining through a wall. *Phys. Rev.*, D92(9):092002, 2015.
- [26] Jonathan L. Ouellet et al. First Results from ABRACADABRA-10 cm: A Search for Sub- μeV Axion Dark Matter. *Phys. Rev. Lett.*, 122(12):121802, 2019.
- [27] V Anastassopoulos, S Aune, K Barth, A Belov, H Bräuninger, Giovanni Cantatore, JM Carmona, JF Castel, SA Cetin, F Christensen, et al. New cast limit on the axion-photon interaction. *Nature Physics*, 13(6):584, 2017.
- [28] Christopher S. Reynolds, M.C. David Marsh, Helen R. Russell, Andrew C. Fabian, Robyn Smith, Francesco Tombesi, and Sylvain Veilleux. Astrophysical limits on very light axion-like particles from Chandra grating spectroscopy of NGC 1275. 7 2019.
- [29] Alexandre Payez, Carmelo Evoli, Tobias Fischer, Maurizio Giannotti, Alessandro Mirizzi, and Andreas Ringwald. Revisiting the SN1987A gamma-ray limit on ultra-light axion-like particles. *JCAP*, 02:006, 2015.
- [30] M. Ajello et al. Search for Spectral Irregularities due to Photon-Axionlike-Particle Oscillations with the Fermi Large Area Telescope. *Phys. Rev. Lett.*, 116(16):161101, 2016.
- [31] Mikhail V. Beznogov, Ermal Rrapaj, Dany Page, and Sanjay Reddy. Constraints on Axion-like Particles and Nucleon Pairing in Dense Matter from the Hot Neutron Star in HESS J1731-347. *Phys. Rev. C*, 98(3):035802, 2018.